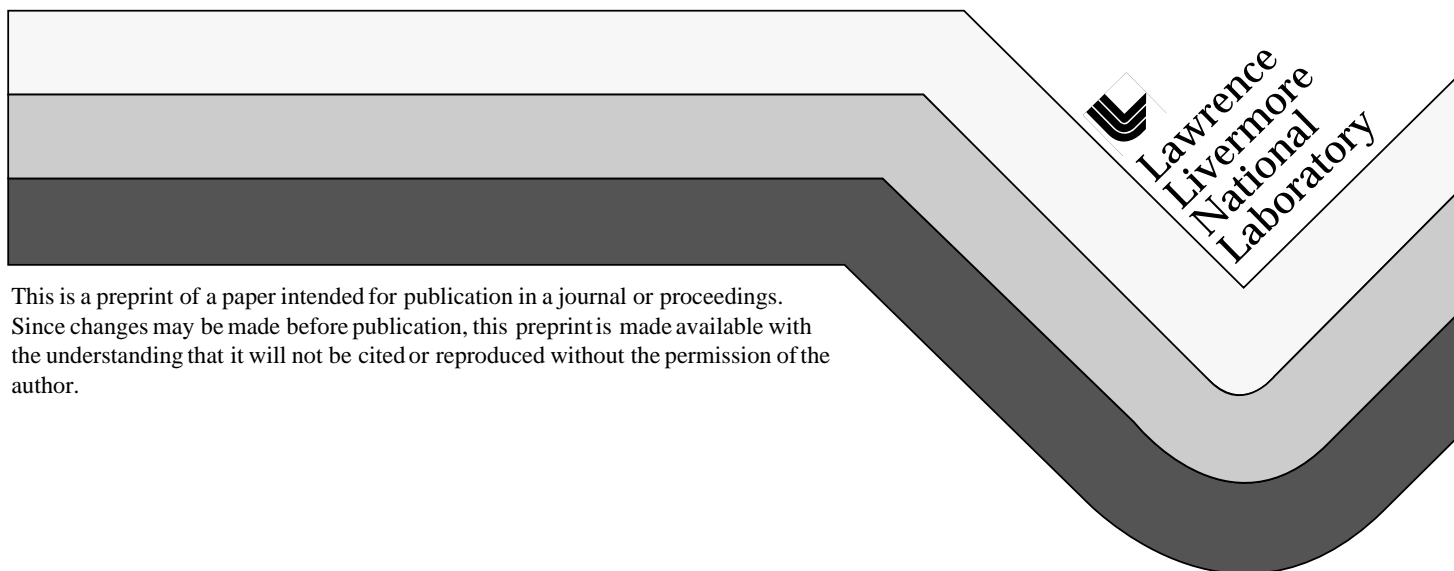


# Passive Films and Blistering of Titanium

Peter J. Bedrossian  
Joseph C. Farmer  
R. Daniel McCright  
Douglas L. Phinney  
John C. Estill

This paper was prepared for submittal to the  
Materials Research Society Fall Meeting  
Boston, MA  
November 28 - December 4, 1998

**December 1998**



#### DISCLAIMER

This document was prepared as an account of work sponsored by an agency of the United States Government. Neither the United States Government nor the University of California nor any of their employees, makes any warranty, express or implied, or assumes any legal liability or responsibility for the accuracy, completeness, or usefulness of any information, apparatus, product, or process disclosed, or represents that its use would not infringe privately owned rights. Reference herein to any specific commercial product, process, or service by trade name, trademark, manufacturer, or otherwise, does not necessarily constitute or imply its endorsement, recommendation, or favoring by the United States Government or the University of California. The views and opinions of authors expressed herein do not necessarily state or reflect those of the United States Government or the University of California, and shall not be used for advertising or product endorsement purposes.

## PASSIVE FILMS AND BLISTERING OF TITANIUM

PETER J. BEDROSSIAN \*, JOSEPH C. FARMER, R. DANIEL McCRIGHT,  
DOUGLAS L. PHINNEY, AND JOHN C. ESTILL  
Lawrence Livermore National Laboratory, Livermore CA 94551  
\*bedrossian1@LLNL.gov

### ABSTRACT

Coupons of titanium alloys under consideration as components of the Engineered Barrier System in the proposed repository at Yucca Mountain have been evaluated for their passive film composition and stability. Oxide depths and compositions on specimens exposed in long-term corrosion testing for one year were determined with x-ray photoemission spectroscopy. The specimens removed from long-term testing, as well as separate coupons polarized cathodically in an electrochemical cell, exhibited blistering associated with hydride formation in both scanning electron microscopy and atomic force microscopy.

### INTRODUCTION

Several commercial grades of titanium are currently under consideration as components of the packages being designed for containment of spent fuel and other high-level waste at the U.S. Monitored Geological Repository planned for Yucca Mountain, Nevada. Table 1 summarizes the compositions of the two titanium alloys investigated in this study.

The addition of Pd to Titanium Grade 16 is believed to raise the corrosion potential of the alloy relative to that of unalloyed titanium. The addition of Mo in Titanium Grade 12 is intended to enhance the passivation of the alloy, while Ni is added to maintain thermodynamic stability.<sup>1</sup>

Table 1: Compositions of Commercial Grades 12 and 16 of Titanium.<sup>2</sup>

ASTM Grade	C (max)	Fe (max)	H (max)	N (max)	O (max)	Ti	Pd	Ni	Mo	Residual Max Total
12	0.08	0.3	0.015	0.03	0.25	bal		0.6-0.9	0.2-0.4	0.4
16	0.08	0.3	0.015	0.03	0.3	bal	0.04-0.08			0.4

These alloys were chosen for their known corrosion resistance, which is considered desirable for a containment application in a repository. Even so, titanium, a strong getter for hydrogen, is known to be susceptible to hydrogen embrittlement.<sup>3, 4</sup> We have therefore initiated a study of hydride formation and swelling in these alloys, employing Secondary Ion Mass Spectrometry (SIMS) to detect hydrogen bound in titanium hydride, and both scanning electron microscopy (SEM) and atomic force microscopy (AFM) to detect swelling and other morphological changes visible on the surface of these alloys following exposure to specific, corrosive conditions.

Corrosion studies for the Yucca Mountain Site Characterization Project have emphasized crevice corrosion as an example of occluded geometries in which the corrosiveness of the electrolyte in the vicinity of the metal barrier might be expected to increase. The presence of crevices is inevitable in the repository. They appear, for example, between the layers of a multiple-layer containment vessel, between a containment vessel and its supports, and between the outer surface of a metal vessel and a silicate scale which may cover it. Under conditions in which oxygen diffusion into a crevice is impeded, metal inside the crevice dissolves anodically, and halide ions migrate into the crevice to balance the resulting excess of positive charge from the titanium cations there. Titanium chlorides are unstable and tend to react with water to form hydrochloric acid and titanium oxide/hydroxide corrosion products, lowering the pH and making the crevice environment increasingly corrosive.<sup>5</sup> Some of the test specimens which underwent long-term testing were configured in a crevice geometry, with the metal sandwiched between teflon washers. Removal of the washers following removal of the specimens from long-term testing permitted direct comparison of the surface chemistry inside and outside the crevices that existed between the metal and the washers.

## EXPERIMENT

The Long-Term Corrosion Test Facility (LTCTF) at Lawrence Livermore Laboratory consists of a collection of tanks filled with recirculating electrolytes of specific, controlled compositions at various temperatures. Table II displays the compositions of the two electrolytes to which samples used in this study were exposed for a period of one year. The electrolytes are synthetic variants of the ground water at Yucca Mountain, and the designations "SCW" and "SDW" represent "simulated concentration well water" and "simulated dilute well water," respectively.

Table II: Compositions of Selected Electrolytes from the LTCTF, in ppm.

	pH	F <sup>-</sup>	Cl <sup>-</sup>	NO <sub>2</sub> <sup>-</sup>	Br <sup>-</sup>	NO <sub>3</sub> <sup>-</sup>	PO <sub>4</sub> <sup>3-</sup>	SO <sub>4</sub> <sup>2-</sup>	Ca <sup>2+</sup>	K <sup>+</sup>	Mg <sup>2+</sup>	Na <sup>+</sup>	Si
SCW	10.3	1370	8810	<10	<20	7740	<70	15700	2	3370	<1	40600	52
SDW	9.9	8	74	<0.1	<0.2	60	<0.7	144	<1	33	<1	440	24

Coupons prepared in a “crevice” configuration were 1/8” thick, 2x2” squares with 3/4”-diameter teflon washers bolted to either side. Crevices then formed between the washers and the metal specimens. The remainder of each coupon was exposed to the electrolyte.

A second set of test coupons was prepared by polishing 5/8”-diameter disks of the titanium alloys with 1/10- $\mu\text{m}$  diamond paste, and then charging them cathodically, at -1.45 V with respect to a saturated calomel electrode, in 1 Molar  $\text{H}_2\text{SO}_4$  at room temperature.

The morphology of the surfaces of the alloys following either removal from the LTCTF or completion of a bench-top polarization experiment was characterized with an SEM (Hitachi 4500) and an AFM (Digital Instruments). Elemental depth profiles were measured with x-ray photoemission spectroscopy (XPS), except for hydrogen which was measured with SIMS.

## RESULTS

Figure 1 displays plots comparing the oxygen concentration, as a function of depth, on a Ti Grade 16 coupon withdrawn from the LTCTF after one year in the SCW electrolyte, as determined by sputter-depth profiling with XPS, together with a similar plot for a control specimen that was never exposed to electrolyte. The sputtering was performed with 4keV Ar ions and was interrupted periodically to record XPS spectra. On both the Grade 12 and Grade 16 coupons, the Ti  $2p_{3/2}$  line appeared at 458.9eV, a position consistent with that of  $\text{TiO}_2$  rather than  $\text{TiO}$ .<sup>6</sup> On both of the grades of titanium tested, the oxide depth inside the crevice was found to be deeper than the oxide depth outside the crevice, as might be expected from the more corrosive environment resulting from the depressed pH inside the crevice.

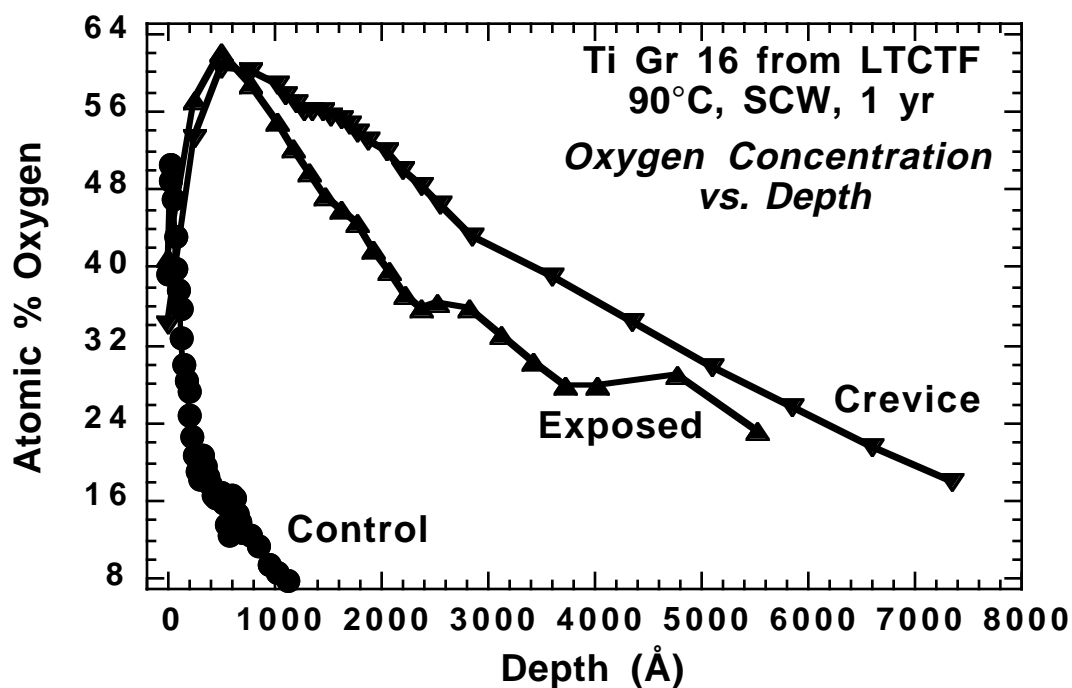


Figure 1: Oxygen depth profile from XPS for Ti Grade 16 crevice coupon from the LTCTF.

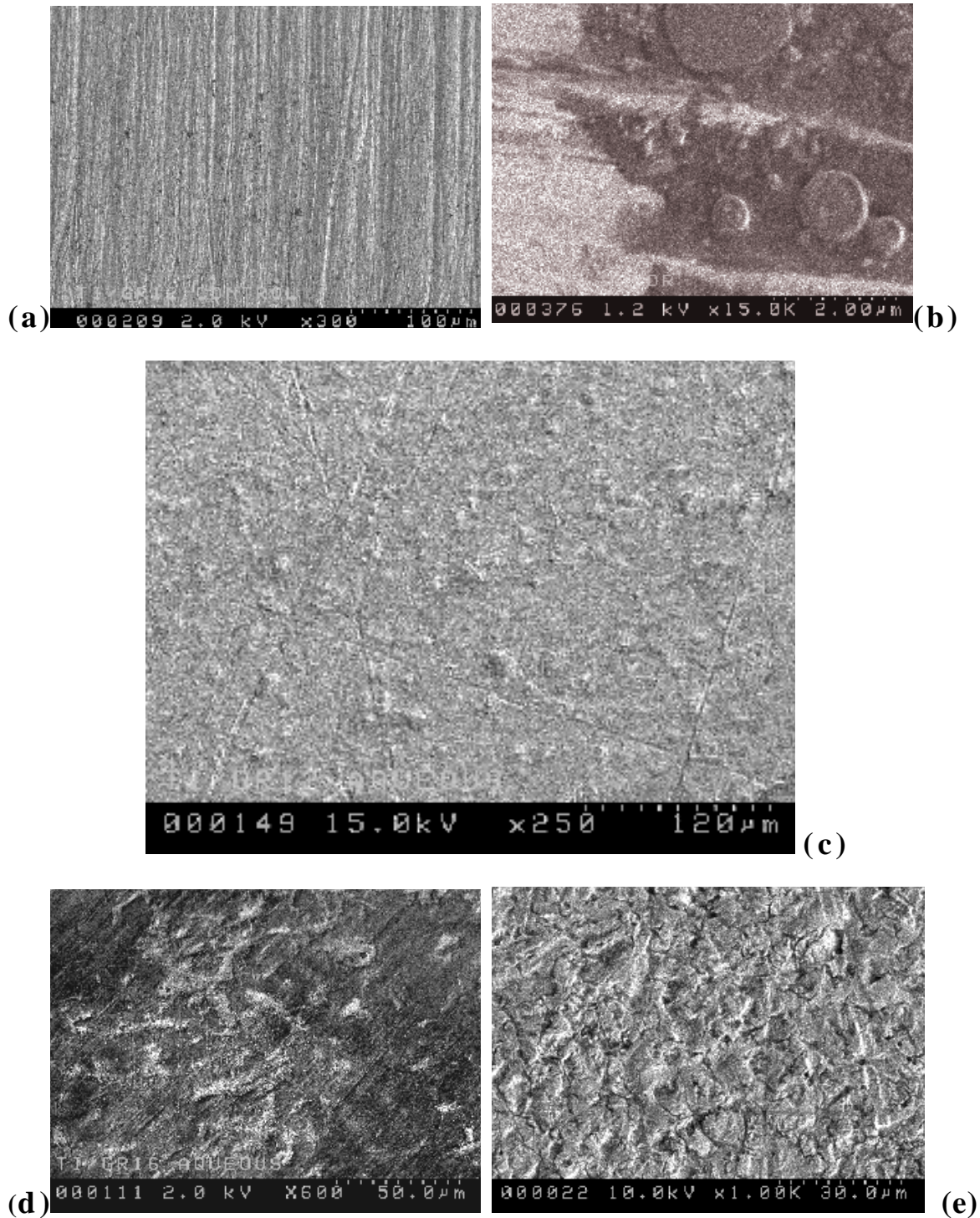


Figure 2: SEM images of coupons exposed to electrolytes for 1 year: displaying (a) an untested coupon of Ti Gr 12, (b) Ti Gr 12 exposed to 60°C SDW, (c) Ti Gr 12, inside a crevice, exposed to 90°C SCW, (d) Ti Gr 16 inside a crevice in the same electrolyte, and (e) Ti Gr 16 outside the crevice in the same electrolyte. Length scales and magnifications are marked below each image.

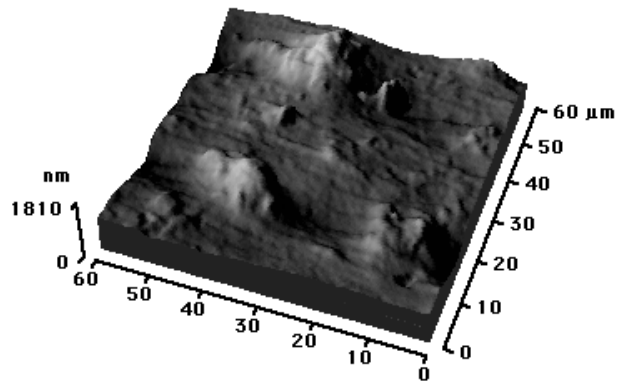


Figure 3: AFM image of Ti Gr 12 inside a crevice, exposed 1 year in 90°C SCW.

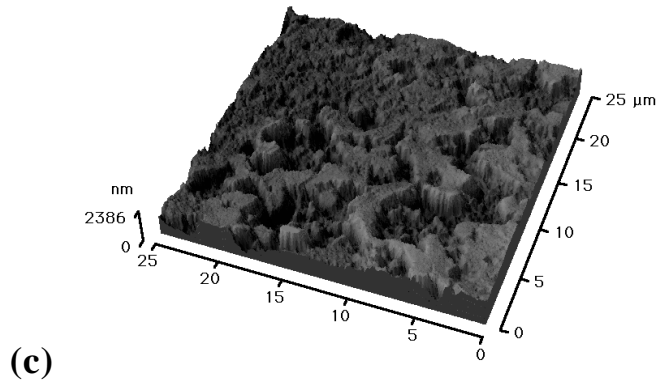
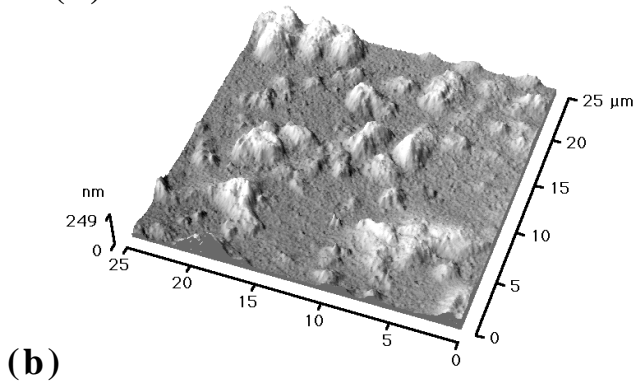
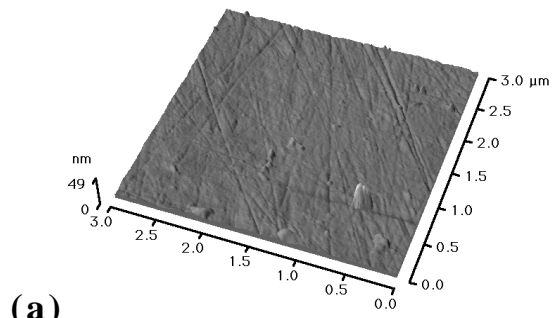


Figure 4: AFM images of Ti Gr 12 cathodically charged as described in text: (a) control, (b) charged 0.25 hours, and (c) charged 24 hours.

Figure 2 displays a set of representative SEM images of Ti coupons removed from the LTCTF one year after their immersion. A control specimen which was never immersed in the electrolyte is shown in Figure 2a, and the other images show features resulting from the corrosion testing which do not appear on the control specimen. Both Grades 12 and 16 of titanium are represented, as are both electrolytes SCW and SDW. Localized swelling in the form of blisters is observed in each case.

Figure 3 displays an AFM image showing a detail of the blisters on the surface displayed in the SEM image in Figure 2c. As shown in the image, the blisters typically rise to heights on the order of a micron above the surrounding substrate.

The localized swelling observed on titanium samples removed from the LTCTF (Figures 2 and 3), is strikingly similar to the morphology observed after cathodic polarization of test coupons in 1M  $\text{H}_2\text{SO}_4$  in an electrochemical cell, as described above. Figure 4 displays AFM images of two test coupons of Grade 12 of titanium following cathodic polarization in the electrolyte. Compared with the control sample, each of the cathodically polarized samples in figure 4 shows enhanced roughness, resulting from swelling, as compared with the relatively smooth, control sample of Figure 4a. Even the brief, 15 minute polarization resulted in blistering shown in figure 4b.

The hydrogen depth profile of each of the cathodically-polarized titanium test coupons was then measured with SIMS. As shown in figure 5, each of the polarized samples has gettered substantially more hydrogen than the control sample. While a reference sample for absolute hydrogen concentration is still in preparation, figure 5 still demonstrates that increasing exposure time in the electrochemical cell is associated with increased hydrogen uptake, for the exposure times used in this study.

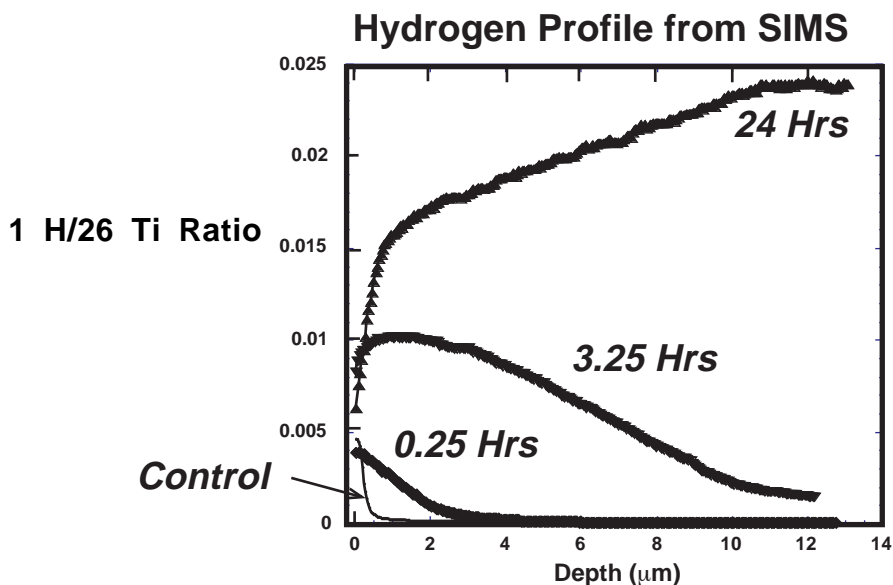


Figure 5: SIMS depth profiles of Ti Gr 12 coupons polarized cathodically in 1M  $\text{H}_2\text{SO}_4$  at room temperature, for the times indicated.



## CONCLUSIONS

We have initiated a series of studies to assess the suitability of certain commercial grades of titanium for inclusion in the Engineered Barrier Systems for the high-level waste repository. Using XPS depth profiling, we have observed enhanced oxidation inside occluded geometries relative to surfaces exposed directly to an electrolyte, on coupons immersed in controlled, aqueous baths in the LTCTF at Lawrence Livermore Laboratory.

Samples of both Titanium Grade 12 and Grade 16 exhibited localized swelling in both SEM and AFM following removal from two distinct electrolytes after 1 year of immersion in the LTCTF. The blistering appearing on these samples is strongly suggestive of similar, localized swelling which appeared on test coupons of Ti Grade 12 polarized cathodically in an electrochemical cell, and which has been shown using SIMS to be associated with hydrogen uptake. The SIMS measurement is insensitive to molecular hydrogen and therefore detects the hydrogen which is in the form of titanium hydride. We plan to apply other types of analysis, including elastic recoil spectroscopy, to measure the total hydrogen uptake in such specimens, because both titanium hydride and dissolved hydrogen may play roles in hydrogen-induced cracking.

## ACKNOWLEDGMENTS

The authors are grateful to D. Delgiudice, C. Evans, and J. Ferreira for technical assistance, and to E. Principe of Charles Evans Associates for a portion of the XPS work. Work was performed under the auspices of the US-DOE at Lawrence Livermore National Laboratory under Contract W-7405-Eng-48. This work is supported by Yucca Mountain Site Characterization Project, LLNL.

## REFERENCES

1. M. Donachie, ed., *Titanium: A Technical Guide*, ASM International, Metals Park, OH, 1988, pp. 207-210.
2. ASTM Designation B 265-95a, "Standard Specification for Titanium and Titanium Alloy Strip, Sheet, and Plate," American Society for Testing and Materials, Philadelphia, PA 1997.
3. D. N. Williams, "The Hydrogen Embrittlement of Titanium Alloys," *Journal of the Institute of Metals* **91**, pp. 147-152 (1962).
4. H. G. Nelson, "Rupture Model of Hydrogen-Induced, Slow Crack Growth in Acicular Alpha-Beta Titanium," *Metallurgical transactions A*, **7A**, pp. 621-627 (1976).
5. R. Boyer, G. Welsch, and E. Collings, ed., *Materials Properties Handbook: Titanium Alloys*, ASM International, Metals Park, OH, 1994, pp. 1070-1073.
6. J. Moulder, W. Stickle, P. Sobol, and K. Bomben, *Handbook of X-ray Photoelectron Spectroscopy*, Physical Electronics Corporation, Eden Prairie, Minnesota, 1992, p. 240.